I J C T A, 9(32), 2016, pp. 165-173 ISSN: 0974-5572

Power Quality Improvement in HVDC Networks Using V2G Technology

D. Bhanuprakash[1], **M. Aruna Bharathi**[2] **and K. Gowthami**[3]

ABSTRACT

Active and passive filters are prerequisites for maintaining power quality in the HVDC network. In this paper active filters based on the trending method in the electric power sector, namely Vehicle to grid (V2G) technology is designed using p-q theory. The results are being compared with the CIGRE benchmark model to demonstrate the low cost solution for the filters in the HVDC system. The potential of a low-cost solution for harmonics is carried out using the PHEV batteries using V2G technology.

Keywords: Vehicle-to-grid (V2G), PHEV, HVDC, Battery, pq theory, Hysterisis

1. INTRODUCTION

The market of Hybrid electric vehicles (HEVs) entering the market has been increasing expeditiously in recent years, since they offer customers a way to increase mileage as they constitute a battery and electric drive system for serving internal combustion engine. HEVs have speed and long distance constraints and they cannot be used effectively.

On the other hand PHEVs has no such constraints. PHEVs can store Electrical energy and they can overcome the difficulties in the HEVs [1]. The strategy of vehicle-to grid (V2G) is implemented by transferring energy from Plug-in Electric Vehicles (PEVs) in a smart grid can support the distribution sector at peak load times. The PEV owners can earn through these power transactions. Grid operating costs can be brought down where the peak time tariffs are high. V2G technology has an ability provide many ancillary services, which includes Reactive power support [1], load leveling [2], spinning reserve and voltage regulation [3], [4], external storage for renewable sources [5], and can provide income to PHEV owners according to load curves [6], [7] thus providing environmental and economic benefits.

An HVDC network is simply a DC transmission system between two AC generating systems. A rectifier inverter group is used for this interfacing. A smart grid comprising HVDC system has been expected in the late eighties and early nineties [9]. However, the snag is the devastating cost of power electronic converters and inverters and their control which were often termed as power electronic devices. From a few past years, many efforts have been made to mitigate these costs and enhance HVDC technology [10-14.] An HVDC transmission system has some major applications compared with AC transmission. An HVDC network is preferred for electric power transmission over long distances and serves best for submarine connections.

In an HVDC network, to reduce harmonics active filters which are a combination of capacitors, power electronic converters, and switching controller, are used [8]. The pricey components of filter or FACTS devices are capacitors. In this work, the capacitors in the filter circuit are substituted with PHEV batteries.

[1,2,3] Sir C.R.Reddy college of Engineering, Eluru, Andhra Pradesh, India, *Emails: bhanu.dasari3@gmail.com, arunabharathi916@gmail.com, gowthami.padma@gmail.com*

The bidirectional charger at the charging station can be served as a converter. A controller is designed using the p–q theory [15].

The use of PHEV as active filter is done in the two configurations:

Case1: PHEV substitution on the rectifier side of the HVDC link.

Case2: PHEV substitution on both the inverter and rectifier sides of the HVDC link.

2. HVDC TEST SYSTEM

The CIGRE model is taken as the base system for addressing harmonics problems which exhibits complex operational characteristics. This benchmark system has a rather simple, but operationally difficult configuration. The values of the main circuit presented are arbitrary and is a two terminal DC scheme. The primary system shown in is a 500 HVDC link which is rated at 1000MW and having 12-pulse converters. The DC line is modeled as a T-network (fig 1).

The control modes are as follows:

At rectifier - constant current control and

At inverter - constant extinction angle control.

Converters in the model are six-pulse Graetz bridge circuits. Each thyristor has a built-in RC snubber circuit. The tuned filters on the rectifier side and the inverter side of the benchmark model are replaced with the PHEVs to obtain a low cost solution and the bidirectional converter is the charging station.

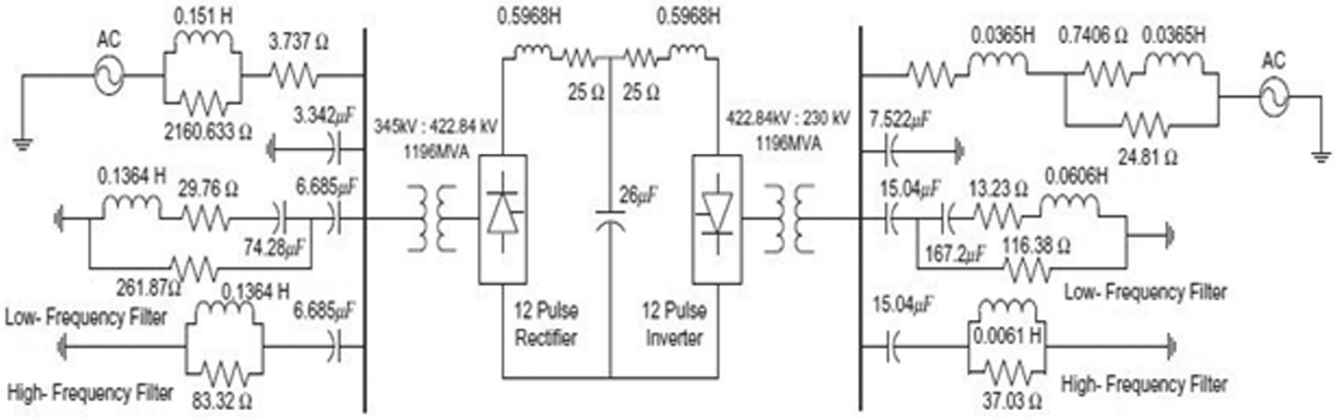

Figure 1: CIGRE benchmark HVDC system

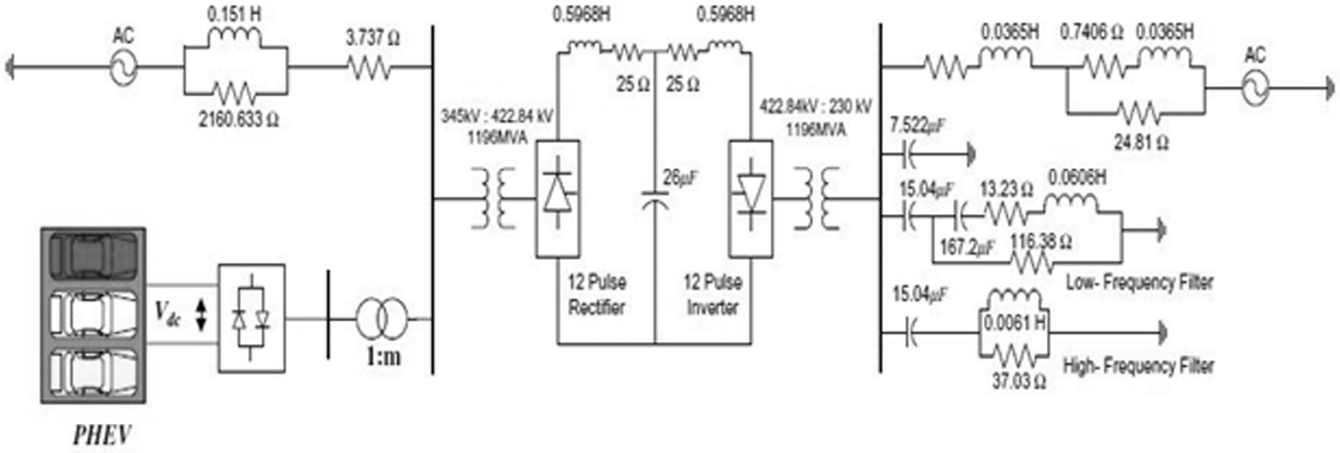

Figure 2: HVDC system with PHEV on rectifier side.

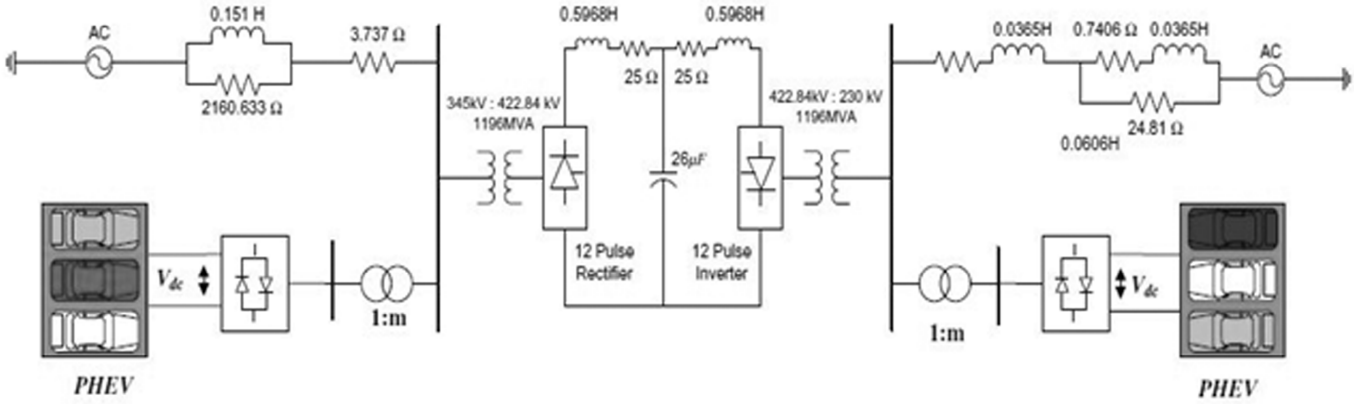

Figure 3: HVDC system with PHEV on both sides

3. PHEV MODELING AND INTERFACING WITH AN HVDC SYSTEM

PHEVs have the capability of compensating the reactive power [16]. In this work, they are considered as bidirectional converters connected dynamic batteries [17]. The P–Q capability of a PHEV varies ±138 kW and between ±126 KVA [16]. Simple battery equivalent with internal impedance is indicated in Fig. 4 . In addition, if the charge efficiency were equal to unity, the charge stored internally as a consequence of a current flowing into the battery would be its integral [18]. This approach has two main issues:

1) The battery characteristics are not practically linear and the battery dynamics are the function of SOC and electrolyte temperature.
2) Charge efficiency cannot be approximated unity.

The other case is the dependence of E on S can be dropped. To handle these constraints, the electric network is modified as indicated in Fig. 5, where, θ represents a measure of the electrolyte temperature.

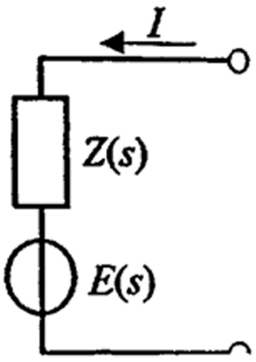

Figure 4: Simple battery equivalent

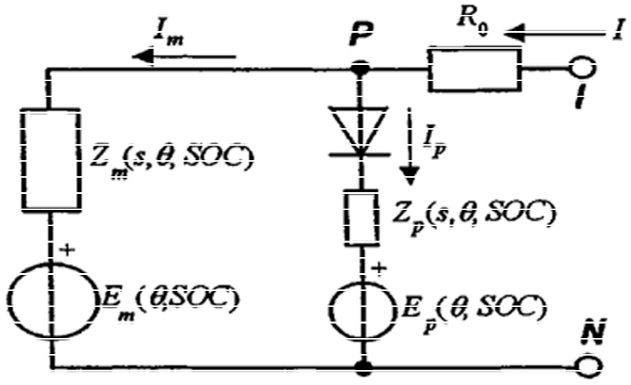

Figure 5: Battery equivalent including parasitic reaction

The third order battery dynamic model is designed taking the current, electrolyte temperature and SOC into consideration and its dynamic equations are:

$$E_m = E_{m0} - K_E(273 + \theta)\ (1\text{-SOC}) \tag{1}$$

$$R_0 = R_{00}[1 + A_0(1\text{-SOC})] \tag{2}$$

$$R_1 = -R_{10}\ln(\text{DOC}) \tag{3}$$

$$R_2 = R_{20}\frac{\exp\left[A_{21}(1-SOC)\right]}{1+\exp\left(A_{22}I_m / I^*\right)} \tag{4}$$

$$\theta = \frac{P_S R_\theta + \theta_a}{1 + R_\theta C_\theta S} \tag{5}$$

The SOC and depth of charge (DOC) can be expressed as

$$SOC = \frac{Q_n - Q_e}{Q_n} = 1 - q \tag{6}$$

$$DOC = 1 - \frac{Q_e}{C\left(I_{avg,}\theta\right)} \tag{7}$$

Here C_θ and Ps are the battery's thermal capacity and power, respectively, R_0 is the thermal resistance and Rp is the polarization resistance, θ_a represents ambient temperature, I* is the reference current, x_r is the Thevenin equivalent reactance, be is the exponential capacity coefficient, Qe is the extracted capacity in Ah, Q_n is the rated battery capacity in Ah and E_m, K_e, K_p, A_0, A_{21} and A_{22} are constants for a battery.

The behavior of the parasitic branch is strongly nonlinear and its current is given as

$$I_p = V_p G_p \exp\left(\frac{V_p}{V_{p0}} + A_p\left(1 - \frac{\theta}{\theta_f}\right)\right)$$

The heat produced by the parasitic reaction can be calculated by means of the Joule law as given by,

$$P_s = R_p I_p^2$$

Where, θ_f is the electrolytic freezing temperature and V_{po}, G_p, and A_p are constants.

A bidirectional converter circuit which is a charger circuit in the real time PHEV charging station is connected to the PHEV to interface with the HVDC link.

4. CONTROLLER ARCHITECTURE

The active controller block is divided into three functional blocks:

4.1. Instantaneous power calculation

PQ theory has been employed for the instantaneous power calculation and is being used for active filter control. We consider the analysis without taking neutral wire into account. The algebraic transformation of the voltage and current components in the abc coordinates to αβ.

The current and voltage equations in αβ coordinates will be

$$\begin{bmatrix} i_\alpha \\ i_\beta \end{bmatrix} = \sqrt{2/3} \begin{bmatrix} 1 & \frac{-1}{2} & \frac{-1}{2} \\ 0 & \frac{\sqrt{3}}{2} & \frac{-\sqrt{3}}{2} \end{bmatrix} \begin{bmatrix} i_a \\ i_b \\ i_c \end{bmatrix} \tag{8}$$

$$\begin{bmatrix} v_\alpha \\ v_\beta \end{bmatrix} = \sqrt{2/3} \begin{bmatrix} 1 & \frac{-1}{2} & \frac{-1}{2} \\ 0 & \frac{\sqrt{3}}{2} & \frac{-\sqrt{3}}{2} \end{bmatrix} \begin{bmatrix} v_a \\ v_b \\ v_c \end{bmatrix} \tag{9}$$

The equation for active and reactive power will be:

$$\begin{bmatrix} p \\ q \end{bmatrix} = \begin{bmatrix} v_\alpha & v_\beta \\ v_\beta & -v_\alpha \end{bmatrix} \begin{bmatrix} i_\alpha \\ i_\beta \end{bmatrix} \tag{10}$$

The main aim of this controller is to calculate the reference values of active and reactive powers by passing the instantaneous values of p and q into a selection block where power is to be compensated (fig 6).

The HVDC link converter behaves like a nonlinear load [19] which voids a fundamental or average and a harmonic or oscillating current component from the power system. The inverse Clarke's transformation is used to approximate the current injected by active filter. To generate the current for controller, Eq. (10) can be written as

$$\begin{bmatrix} i_\alpha \\ i_\beta \end{bmatrix} = \frac{1}{v_\alpha^2 + v_\beta^2} \begin{bmatrix} v_\alpha & v_\beta \\ v_\beta & -v_\alpha \end{bmatrix} \begin{bmatrix} p \\ q \end{bmatrix} \tag{11}$$

4.2. Power Compensation section

The p and q values can be separated into average and oscillatory parts for our convenience.

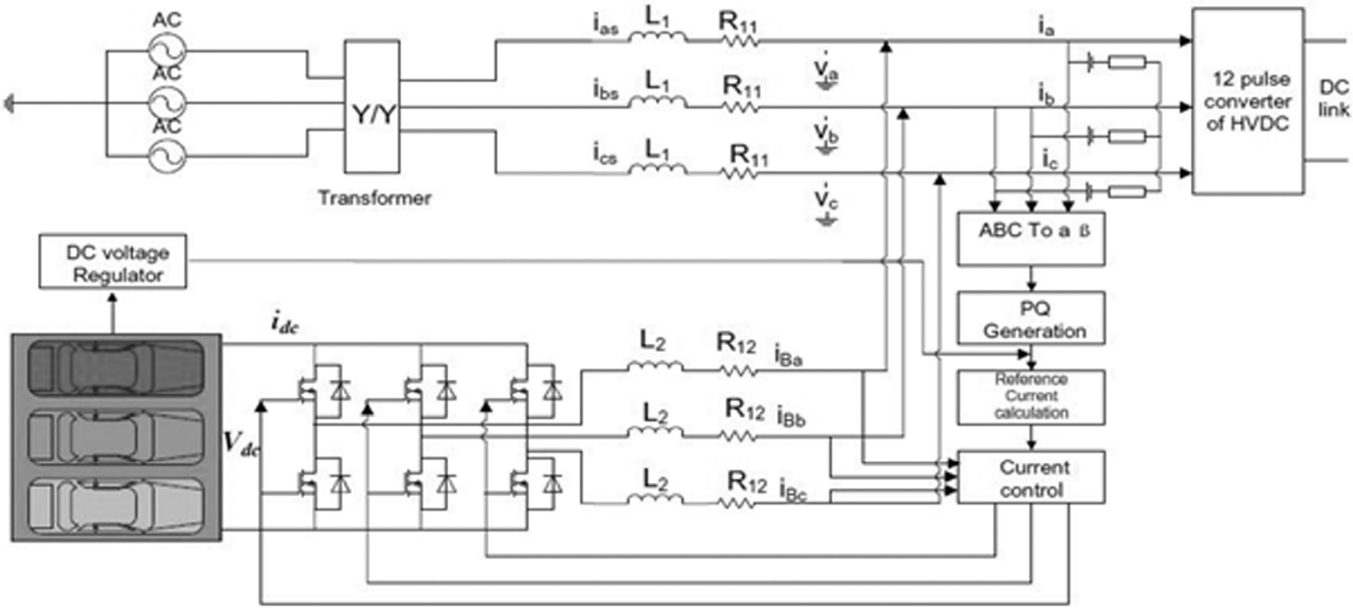

Figure 6: Main control circuit

$$p = \bar{p} + \tilde{p} \tag{12}$$

$$q = \bar{q} + \tilde{q} \tag{13}$$

The αβ variables defined in Eq. (10) are replaced with equivalent expressions referred to the abc axis using Eq. (8) and similarly for the current, the following relationship can be found:

$$p = v_\alpha i_\alpha + v_\beta i_\beta$$

$$p = \frac{1}{3}\left[\left\{\left(v_a - v_b\right) - \left(v_c - v_a\right)\right\} i_a + \left\{\left(v_b - v_c\right) - \left(v_a - v_b\right)\right\} i_b + \left\{\left(v_c - v_a\right) - \left(v_b - v_c\right)\right\} i_c\right]$$

$$= \frac{1}{3}\left[\left(v_{ab} - v_{ca}\right) i_a + \left(v_{bc} - v_{ab}\right) i_b + \left(v_{ca} - v_{bc}\right) i_c\right] \tag{14}$$

And,

$$q = v_\beta i_\alpha + v_\alpha i_\beta$$

$$= \frac{1}{\sqrt{3}}\left[\left(v_a - v_b\right) i_c + \left(v_b - v_c\right) i_a + \left(v_c - v_a\right) i_b\right]$$

$$= \frac{1}{\sqrt{3}}\left(v_{ab} i_c + v_{bc} i_a + v_{ca} i_b\right) \tag{15}$$

The compensating current is given by,

$$\begin{bmatrix} i_{com\alpha} \\ i_{com\beta} \end{bmatrix} = \frac{1}{v_\alpha^2 + v_\beta^2} \begin{bmatrix} v_\alpha & v_\beta \\ v_\beta & -v_\alpha \end{bmatrix} \begin{bmatrix} -\breve{p} + P_L \\ -q \end{bmatrix}$$

Where, P_L is the power from DC voltage regulator and helps to maintain V_{dc} around the reference value. If the AC voltage is greater than the DC voltage, the PWM controller loses its controllability, in this case the rating of DC capacitor need to be large. However PHEV Park serves this need.

4.3. DC voltage regulation and the current controller

In this work, Hysteresis controllers have been used since, they offer robust and smooth operation [20]. A dynamic offset (ε) is created from the measurement of Vdc and the DC reference voltage in such a way that upper and lower band limits of the hysteresis current controller are $i_{ref} + \Delta(1 + \in)$ and $i_{ref} - \Delta(1 + \in)$ respectively.

5. SIMULATION RESULTS

5.1. PHEV filter on rectifier side

Analyses have been carried out for the performance check. A real time harmonics spectrum is analyzed, and it is determined that it's different orders have the maximum and minimum levels of 0.31% and 0.05% magnitude respectively as shown in fig 7. The THD value in the transient state and steady state are traced out and their values are 4.4% and 0.2 respectively as shown in fig 8. which are acceptable according to the IEEE standard 519 [21].

5.2. PHEV filter on both sides

The tuned filters on both sides of the CIGRE model are replaced by the PHEV batteries. The results are taken on the inverter side of the HVDC link. The maximum and minimum levels of harmonic currents are

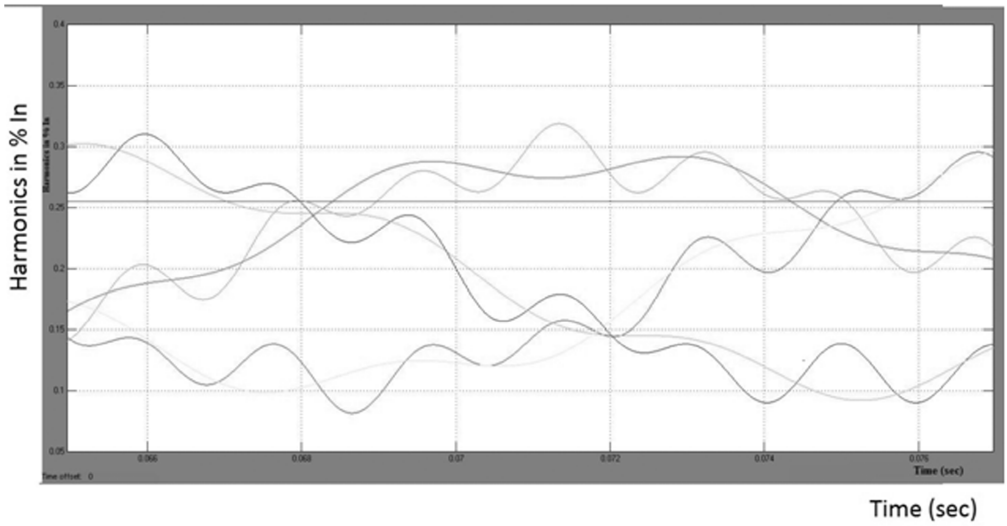

Figure 7: Harmonics currents (case 1)

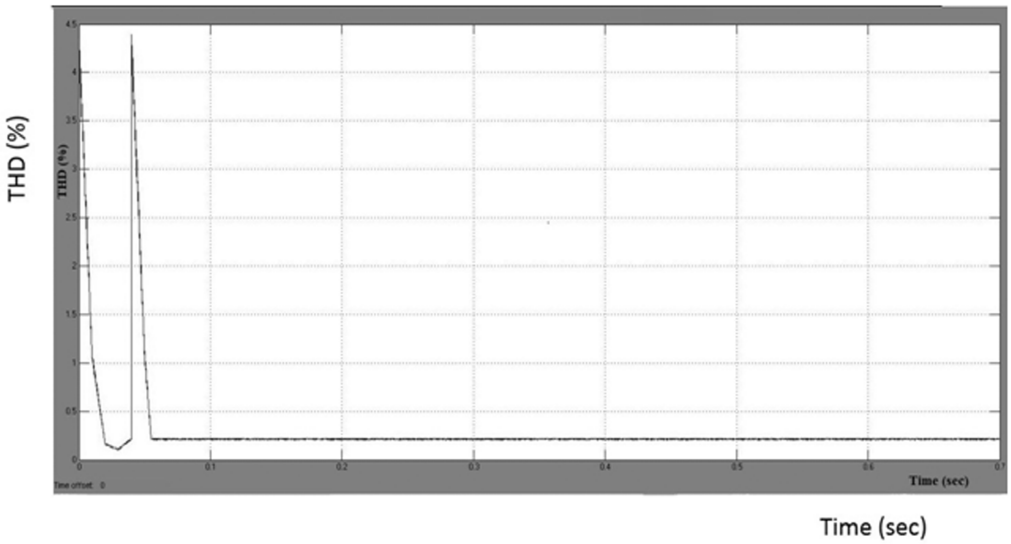

Figure 8: THD analysis (case 1)

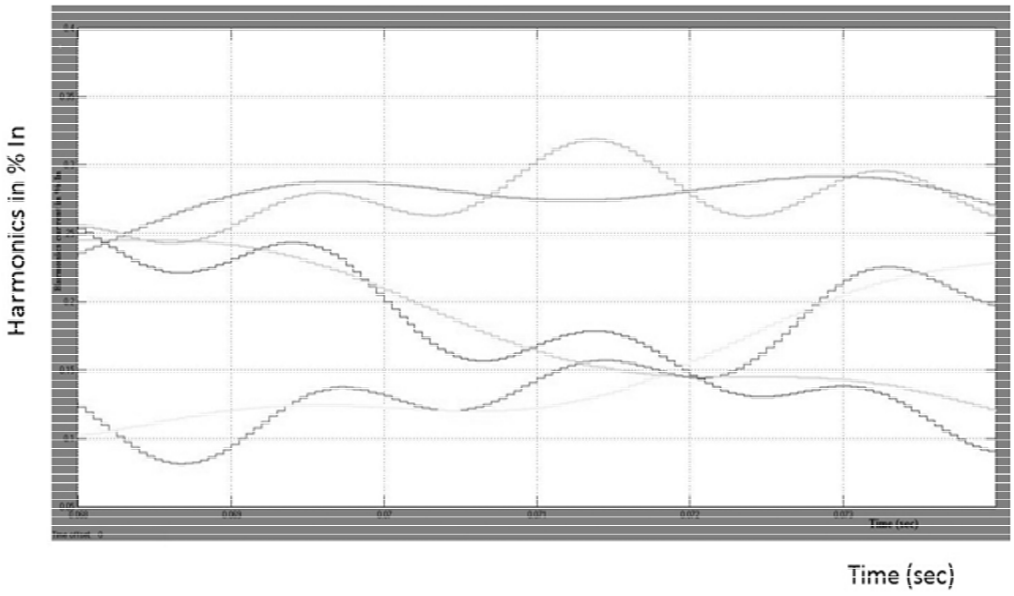

Figure 9: Harmonic currents(case 2)

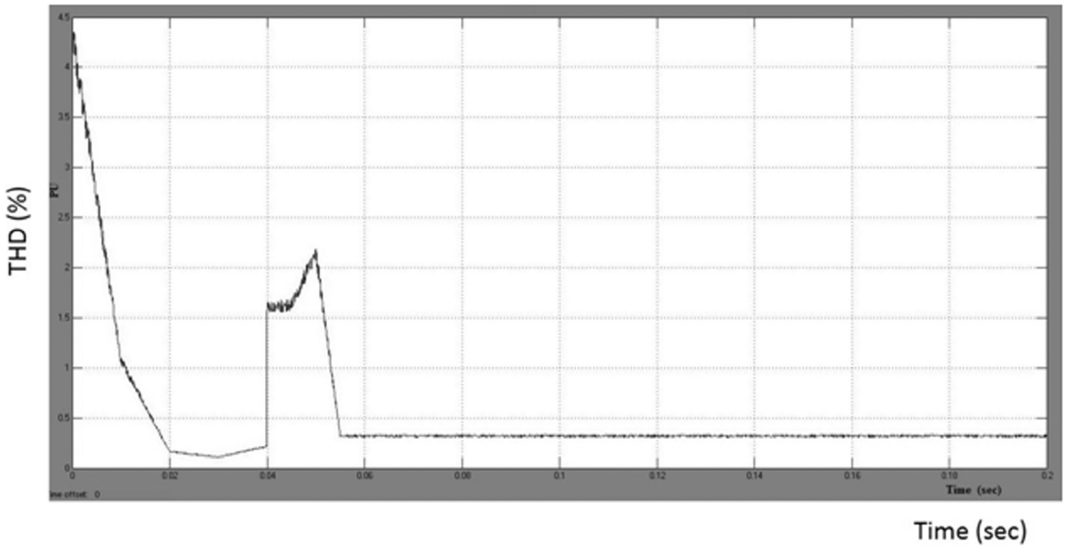

Figure 10: THD analysis (case 2)

0.33% and 0.08% (fig 9). The THD of the Inverter current in transient state and steady state are 4.45% and 0.4% respectively as shown in fig 10.

REFERENCES

[1] M. C. Kisacikoglu, B. Ozpineci, and L. M. Tolbert, "Examination of a PHEV bidirectional charger system for V2G reactive power compensation," in *Proc. 2010 25th Annu. IEEE Appl. Power Electron. Conf. Expo. (APEC)*, pp. 458–465.

[2] C. Guille and G. Gross, "A conceptual framework for the vehicle- to-grid (V2G) implementation," *Energy Policy*, vol. 37, no. 11, pp. 4379–4390, Nov. 2009.

[3] W. Kempton and J. Tomic, "Vehicle-to-grid power fundamentals: Calculating capacity and net revenue," *J. Power Sources*, vol. 144, no. 1, pp. 268–279, Jun. 2005.

[4] J. Tomic and W. Kempton, "Using fleets of electric drive vehicles for grid support," *J. Power Sources*, vol. 168, no. 2, pp. 459–468, Jun. 2007.

[5] W. Kempton and J. Tomic, "Vehicle-to-grid power implementation: From stabilizing the grid to supporting large-scale renewable energy," *J. Power Sources*, vol. 144, no. 1, pp. 280–294, Jun. 2005.

[6] A. Y. Saber and G. K. Venayagamoorthy, "Intelligent unit commitment with vehicle-to-grid—A cost-emission optimization," *J. Power Sources*, vol. 195, no. 3, pp. 898–911, Feb. 2010.

[7] C. Hutson, G. K. Venayagamoorthy, and K. Corzine, "Intelligent scheduling of hybrid and electric vehicle storage capacity in a parking

[8] Gunnarsson Stefan, Jiang L, Petersson Anders. Active filters in HVDC transmission. http://www.abb.com/HVDC lot for profit maximization in grid power transactions," in *Proc. IEEE Energy 2030*, Nov. 17–18, 2008, pp. 1–8.

[9] Laughton MA, Warne D, editors. Electrical engineer's reference book. Elsevier; 2003.

[10] IEEE guide for the evaluation of the reliability of HVDC converter stations, IEEE Std 1240-2000; 2001.http://dx.doi.org/10.1109/IEEESTD.2001.245621.

[11] Agelidis V, Demetriades G, Flourentzou N. Recent advances in high voltage direct current power transmission systems. In: IEEE international conference on industrial technology; 2006. p. 206 13.

[12] Flourentzou N, Agelidis V, Demetriades G. VSC based HVDC power transmission systems: an overview. IEEE Trans Power Electr 2009; 24(3): 592–602.

[13] Zhang X, Bai J, Cao G, Chen C. Optimizing HVDC control parameters in multi in feed HVDC system based on electromagnetic transient analysis. Int J Electr Power Energy Syst 2013;49:449–54.

[14] Kili U, Ayan K. Optimizing power flow of AC–DC power systems using artificial bee colony algorithm. Int J Electr Power Energy Syst 2013;53:592–602.

[15] Akagi H, Watanabe E, Aredes M. Instantaneous power theory and applications to power conditioning. Willey Interscience; 2007.

[16] Mitra P, Venayagamoorthy G, Corzine K. Smart Park as a virtual STATCOM. In: IEEE trans on smart grid 2011;2(3):445–455.

[17] Kisacikoglu M, Ozpineci B, Tolbert L. Examination of a PHEV bidirectional charger system for V2G reactive power compensation. In: Applied power electronics conference and exposition (APEC21); 2010. p. 458–65.

[18] Ceraolo M. New dynamical models of lead-acid batteries. IEEE Trans Power Syst 2000;15(4):1184–90.

[19] Singh A Singh B. Performance evaluation of power converters with distribution static compensator. In: Joint international conference on power electronics, drives and energy systems (PEDES 2010) India; 2010. p. 1–5

[20] Tilli A, Tonielli A. Sequential design of hysteresis current controller for three phase inverter. IEEE Trans Ind Electr 1998;45(5):771–81.

[21] IEEE Std 519-1992, IEEE Recommended Practices and Requirements for Harmonic Control in Electric Power Systems_ Institute of Electrical and Electronics Engineers, Inc.; 1993.